# *Experimental Investigation of Superelasticity Degeneration and Plastic Yielding Behavior of Ni–Ti Shape Memory Alloys*

**Ran Li [1, a,*], Zhen Liu[2, b]**

[1]*School of Civil Engineering, Southeast University, Nanjing 211189, China*
[2]*East China Architectural Design & Research Institute, Shanghai 200002, China*
[a] *li-liran@163.com,* [b] *230129152@seu.edu.cn*

***Keywords:*** Shape memory alloy, superelasticity degeneration, plastic yielding, cyclic loading.

***Abstract:*** Cyclic loading tests on superelastic and plastic yielding shape memory alloy (SMA) wires are conducted to investigate the phenomena of superelasticity (SE) degeneration and plastic yielding. Parameters influencing the mechanical properties of SMAs are investigated and the variation tendencies of the mechanical properties are discussed. The results indicate that both the SE degeneration and the plastic yielding in SMA wires are affected by the cyclic numbers; The plastic yielding SMA wire exhibits severe SE degeneration and plastic yielding phenomena; Superior SE is demonstrated in the superelastic SMA wire.

## 1. Introduction

Shape memory alloys (SMAs), which possess unique mechanical and physical properties, are used in many fields including aerospace, biomedical and civil engineering. Certain SMAs have excellent superelasticity (SE), durability, and fatigue performance. Recently, both experimental studies and finite element analytical simulations have been conducted by researchers on applications of energy dissipation and vibration isolation in civil engineering.

The martensite phase occurs when the loading stress exceeds the elastic limit of an austenite SMA at ambient temperature. During unloading, the martensite phase disappears as the stress decreases and the SMA is restored to its initial state. This phase transition is called the superelastic effect. Plastic yielding occurs when the stress exceeds the plastic yielding stress; the large residual strain remains in the material even if the stress drops to zero.

Many researches about the SE of SMAs in the application of civil engineering have been conducted [1,2]. The SE of SMAs can be applied to develop various damping devices for structural vibration control [3]. In addition, studies of the correlation between SE and strain amplitude have been conducted [4,5]. The phenomena during the testing process indicated that different mechanical




DOI: 10.23977/msmee.2018.72135

properties, such as the SE and the plastic yielding, could appear. In order to maintain the SE, the martensitic transformation start stress of SMA should not exceed the yielding stress ($M_s \leq \sigma_{fy}$). However, few researchers focus on the plastic yielding phenomenon.

In this study, two groups of SMA wires are tested by cyclic loading. The effects of the cycle number and strain amplitude on the SE and plastic yielding of SMAs are studied. The influences on the mechanical behaviors, including the residual strain, peak stress, and energy dissipation capacity of SMAs are investigated. The results provide a test basis and theoretical foundation for the application of SMAs in structural vibration control devices.

## 2. Mechanical Behavior Test of SMA Wire

### 2.1 Testing Specimen

The sample diameter of SMA was 1.0 mm with the alloy composition of Ti-55.84 wt.% Ni. The specimens were 130 mm in length with a gauge length of 60 mm. The four phase transition temperatures were $M_f$=-47.5°C, $M_s$=-26.3°C, $A_s$=-15.2°C, and $A_f$=-3.2°C, respectively, which were obtained by differential scanning calorimetry method. Then, the specimens used for the experimental tests were austenite at room temperature (20°C).

To investigate the SE and the plastic yielding of the SMA, two groups of SMA wires were selected to investigate the SE and the plastic yielding of the SMA; Group P was the plastic yielding group and Group S was the SE group. Group P and Group S were each divided into two cases. The case number and the loading programs are listed in Table 1.

Table 1 Test cases and loading conditions

| Test case | $N$ | $\varepsilon_{amp}$ (%) | $T$ (°C) | Test case | $N$ | $\varepsilon_{amp}$ (%) | $T$ (°C) |
|---|---|---|---|---|---|---|---|
| P-I | 20 | 7 | 20 | S-I | 20 | 7 | 20 |
| P-II | 1 | 1, 2, 3, 4, 5, 6, 7 | 20 | S-II | 1 | 1, 2, 3, 4, 5, 6, 7 | 20 |

### 2.2 Testing Result

Fig. 1 shows the stress–strain curves of the two groups with different loading cases. As shown in Fig. 1(a-1), residual strain of about 0.25% is left in the first cycle. However, the residual strain increases sharply with an increment of 1%. Then, this increment decreases slowly with increased cyclic number. Moreover, the transverse transformation and reverse transformation points become less obvious and the austenite and martensite moduli gradually decrease. The hysteretic curves become long and narrow, and gradually stabilizes as a willow-leaf shape. Significant SE degeneration appears in the testing process. In Fig. 1(a-2), the residual strain, which is far lower than that of Group P, increases slowly and then reaches to a steady state. The stress–strain curves show flag-shaped hysteretic curves with obvious start and finish points of the phase transformation. The austenite and martensite moduli change little with increased cyclic number. The start and finish phase transformation stresses are decreased with increased cycle number; the reduction of the transverse transformation is larger than that of the reverse transformation. In addition, both the residual strain and the phase transformation points tend towards stability. A steady SE is reached and no obvious SE degeneration appears with increased cycling.

Fig. 1(b) gives the stress–strain curves of P-II and S-II at different strain amplitudes. Seen from Fig. 1(b-1), no visible phase transformation point occurs in the P-II test (Fig. 6(a)) throughout the process. The maximum stress increases with increasing strain amplitude, and strengthening occurs at

strain amplitudes between 4% and 5%. Conspicuous plastic yielding occurs after strengthening and the increment of the residual strain becomes larger. For the S-II test, shown in Fig. 1(b-2), exhibits significant differences from that of the P-II test. The four phase transformation points are noticeable. All residual strains are almost zero in each cycle after unloading, which indicates that the SMA wire of the Group S have better SE than that of the Group P.

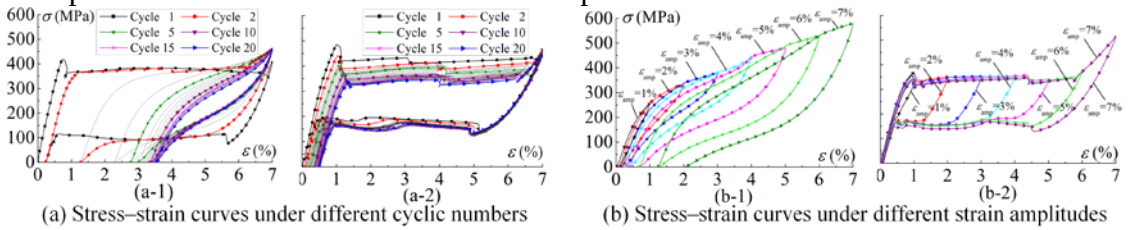


(a) Stress–strain curves under different cyclic numbers (b) Stress–strain curves under different strain amplitudes

Fig. 1 Stress–strain curves of the SMA under different loading cases

## 3. Analysis and Discussion

In a macroscopic view, the SE degeneration of the SMA can be described by the increment and accumulation of residual strain, while the plastic yielding of the SMA is described by the peak stress. In order to analyze the influences of the cycle number $N$ and the strain amplitude $\varepsilon_{amp}$ on the SE and plastic yielding behavior, the variations of residual strain $\varepsilon_{res}$, and peak stress $\sigma_{max}$ are analyzed.

### 3.1 Effect of Cyclic Number N

Fig. 2 shows the influence of cyclic number $N$ on the SE and plastic yielding properties of the two groups of wires. Shown in Fig. 2(a) are the residual strains and energy dissipation of the two groups of wires with increasing cycle number $N$. Large increments in the residual strain of the Group P are retained after the first five cycles, and the maximum increase in the residual strain appears at the end of the second cycle. The increases gradually shrink, then approaching a stable state in the last several cycles. The stress–strain curve of the Group S grows gently with a small residual strain in each cycle. The cumulative residual strain of the Group S in the twentieth cycle is only 0.507%, while that of the Group P is measured as 3.533%, 6.97 times greater than that of the Group S.

The energy dissipation of both groups of wires displays declining tendencies under increased cycling, as shown in Fig. 2(a). The energy dissipation of Group P in the third cycle is sharply decreased compared to that of the second cycle. The decline tendency becomes gentler after five cycles, and stabilizes after fifteen cycles. The energy dissipation of Group S decreases with increased cycling without severe variation. It gradually stabilizes after fifteen cycles. The energy dissipation of the two groups at the twentieth cycle are 1745 J/mm$^3$ and 7598 J/mm$^3$, respectively. The cyclic dissipations decrease to 12.89% and 70.76% at the last cycle comparing to those of the first cycles for the two groups. The steady-state energy dissipation of the Group S is approximately 4.56 times that of the Group P.

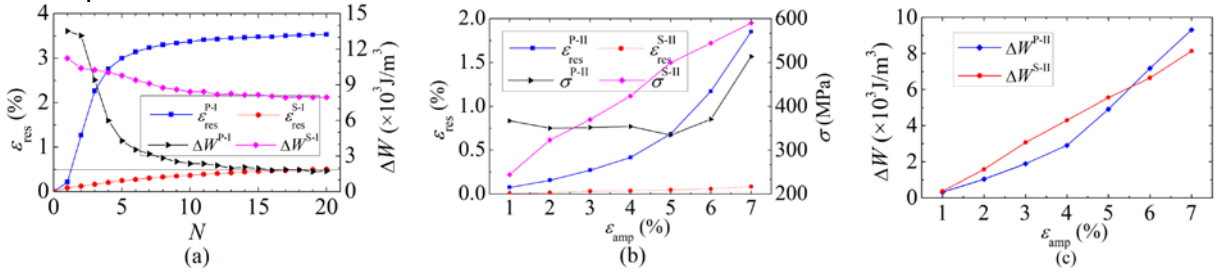


Fig. 2 Effect factors on SMA properties: (a) cyclic number, (b)&(c) strain amplitude

The main reason of the decreased energy dissipation in the Group P is the increasing residual strain; while the main cause of the SE degeneration of the Group S is the decrease in phase transformation stress. Regarding microscopic factors, the high local stress near the austenite– martensite interfaces could cause dislocation slippage. Such slippage near austenite–martensite interfaces could prevent the reverse transformation process. The density of the dislocation slippage increases quickly with increased cycling, thereby severely decreasing the SE [6].

### 3.2 Effect of Strain Amplitude εamp

Fig. 2(b) depicts the influence of the strain amplitude on the residual strain and peak stress. The residual strain of the Group P increases rapidly and the increment of which becomes larger as the strain amplitude increases. The residual strain of the Group S increases slightly. The residual strains of the Group P and Group S are 0.417% and 0.037%, respectively, at $\varepsilon_{amp}$=1%. The value of Group P is 11.27 times greater than that of Group S. The residual strains are 1.852% and 0.085%, respectively, at $\varepsilon_{amp}$=7%; the former is 21.81 times greater than the latter.

The peak stress of the Group P linearly increases with increasing strain amplitude The peak stress of the Group S exhibits two stages, first remaining steady before increasing suddenly. The stress is approximately 350 MPa at strain amplitudes of 5% or less. Notably, the stress amplitude at the strain amplitude of 1% is somewhat larger than that at other strain amplitudes. As shown in Fig. 1(b-2), the austenite elastic stage finishes near the strain amplitude of 1%, at which point the martensitic transformation begins. The dislocation slippage in this material and the high local stress near the austenite–martensite interfaces cause macroscopic increases in the stress amplitude increment. The peak stress decreases only slightly at $\varepsilon_{amp}$=5%. This might be caused by local stress release. An inflection point appears when the strain amplitude increases from 5% to 6% because the martensitic transformation finishes near the strain amplitude of 5.7%, as shown in Fig. 1(b-2). The peak stress increases linearly when the strain amplitude is increased from 6% to 7%, because the martensitic elastic deformation of the material dominates during this stage.

It is clear that the cyclic energy dissipations of the two groups of SMAs are increased with increasing strain amplitude, as shown in Fig. 2(c). The energy dissipation trend of the Group P displays a convex tendency early, and then increases linearly. The reason is that the material experiences a strengthen process (Fig. 1(b-1)) under strain amplitudes larger than 4.5%. For the Group S, the energy dissipation increases approximately linearly.

From a macroscopic view, plastic deformation occurs before the phase transformation starts, which increases the relative residual strain. For the Group S, negligible residual strain remains because of the SE. In microscopic factors, the martensitic–austenitic transformation occurs incompletely during unloading, and the residual martensite contributes to the residual strain. During the loading process, internal stress can be induced by the increased dislocation density, and may assist the nucleation of stress-induced martensite phases. The dislocation slippage near the interface of the two phases can prevent the denucleation of the martensite.

## 4. Conclusion

Two groups of Ni-Ti SMA wires with different properties (i.e., SE degeneration and plastic yielding) are compared through experiments. The stress–strain relationships of the two groups of wires under variations in parameters like cyclic number, and strain amplitude are proposed. The residual strain, peak stress, and energy dissipation per cycle are also investigated. The results of this study establish a foundation for describing the mechanical behaviors. Conclusions are summarized as follows:

1) A flag-shaped hysteretic curve is obtained in the Group S during the loading process at room temperature. The energy dissipation and the peak stress increase linearly with increased strain amplitude. It exhibits good energy dissipation capacity with small residual strain during the loading process, and no obvious SE degeneration occurs.

2) Stress strengthening occurs in SMA wires of the Group P during the loading process at room temperature. The energy dissipation of this group is weak. The SE degenerates severely with a large residual strain. The energy dissipation capacity increases with increased strain amplitude; however, the residual strain also increases rapidly.

## Acknowledgments

This study is supported in part by Priority Academic Program Development of Jiangsu Higher Education Institutions, China (PADA NO. 1105007002).

## References

*[1] H. W. Ma and C. H. Yam. Experimental study on a beam-to-column connection using shape memory alloy. Advanced Materials Research, 2012, 374-377, 2176-2179.*

*[2] M. R. Eatherton, L. A. Fahnestock and D. J. Miller. Computational study of self-centering buckling-restrained braced frame seismic performance. Earthquake Engineering & Structural Dynamics, 2014, 43, 1897-1914.*

*[3] W. J. Ren, L. Q. Wang, Z. C. Ma, et al. Investigation on mechanical behavior of innovative shape memory alloy-friction damper. Journal of Building Structures, 2013, 34(2), 83-89.*

*[4] L. Janke, Czadershi C Motavalli M and Ruth J. Application of shape memory alloys in civil engineering structures-Overview, limits and new ideas. Materials and Structures, 2005, 38, 578-592.*

*[5] O. E. Ozbulut. Seismic protection of bridge structures using shape memory alloy-based isolation systems against near-field earthquakes. Texas A&M University, 2010.*

*[6] R. Delville, B.Malard, J. Pilch, P. Sittner, D. Schryvers. Transmission electron microscopy investigation of dislocation slip during superelastic cycling of Ni-Ti wires. International Journal of Plasticity, 2011, 27(2), 282-297.*